A Comprehensive Case Study of the Frio CO_2 Sequestration Pilot Test for Safe and Effective Carbon Storage Including Compositional Flow and Geomechanics

Hojung Jung, D. Nicolas Espinoza, Gurpreet Singh and Mary F. Wheeler

2016 Mastering the Subsurface through Technology Innovation and Collaboration: Carbon Storage and Oil and Natural Gas Technologies Review Meeting

Introduction

Carbon dioxide (CO_2) geological sequestration is a direct method to reduce carbon emission to the atmosphere by injecting CO_2 into deep geological structures. Deep geological structures include depleted oil and gas reservoirs and saline aquifers. In-depth understanding of the long-term fate of stored CO_2 requires study and analysis of the reservoir formation, the caprock formation, and the adjacent faults. This poster shows an example of a combination of carefully conceived laboratory experiments, upscaling, and numerical simulation of long-term storage of CO_2 in the Frio injection site.

Objective

This research investigates long term effects of CO_2 injection regarding secure and permanent CO_2 storage by conducting experiments, analyzing well logs and performing numerical reservoir simulation. The experiments include measurement of petrophysical and geomechanical properties of Frio rocks subjected to CO_2 and CO_2-acidified water at in-situ stress condition. These measurements seek to characterize the relative magnitude of chemical couplings with geomechanics as well as typical flow properties. Finally, the measured parameters are employed in a computational geomechanical screening tool that considers the risk associated with CO_2 sequestration.

Frio C Sand

Frio formation is a saline aquifer in East Texas in which two pilot tests of CO_2 sequestration were conducted (Hovorka et al., 2006). Figure 1 shows the geological strata of Frio formation, and it is composed of sands with highly bedded shale layers. Frio sandstone cores are retrieved from the pilot test site and are available from the Houston Research Center (Figure 2, BEG – The University of Texas, Austin).

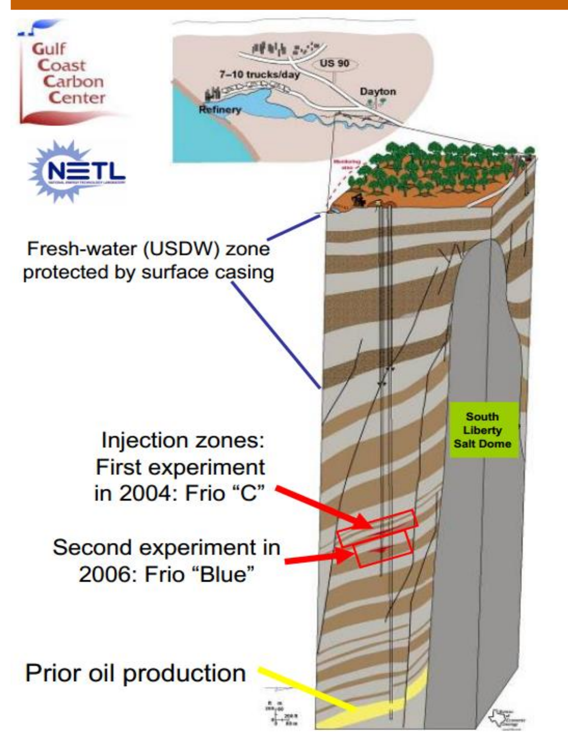

Fig. 1. Schematic of a Frio formation geological strata (Hovorka, GCCC)

Fig. 2. Frio sandstone cores provided by (BEG-UT Austin)

Triaxial loading cell and fluid injection system

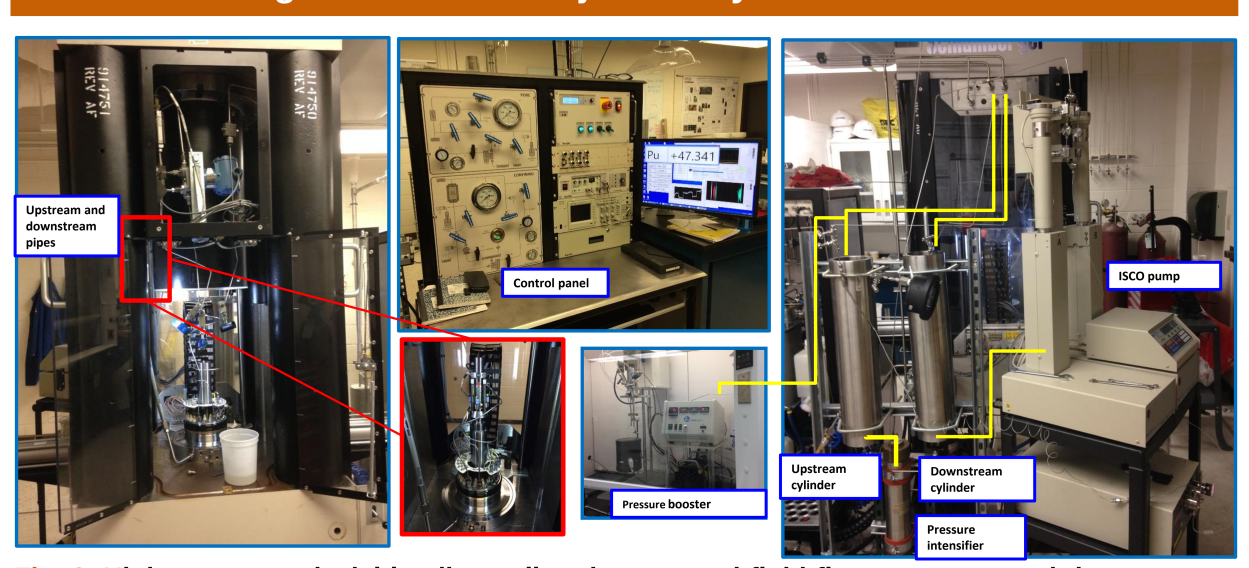

Fig. 3. High-pressure triaxial loading cell and connected fluid flow upstream and downstream system

Summary of accomplishments to date

- Elastic and inelastic mechanical properties are accurately measured by multistage triaxial loading test and Biot coefficient loading test. The results show typical behavior of unconsolidated sand, and the analyzed mechanical properties are applied to calibrate well logs analysis.
- Basic and advanced petrophysical properties are evaluated under the reservoir stress condition. The measured properties are carefully matched with the well logging analysis results.
- Finally, all the calculated petrophysical properties are implemented into a compositional reservoir simulator, and the simulation results show reasonable pressure transient.

References

- Hovorka, S.D., C. Doughty, S.M. Benson, and others, (2006). Measuring permanence of CO_2 storage in saline formations: The Frio experiment, Environ. Geosci., 13(2): 105–121.
- Hovorka, S.D. (2009) – Frio Brine Pilot: the First US Sequestration Test.
- Bouteca, M., Sarda, J.P., Vincke, O., & Longuemare, P. (1999). Thoughts about the micro-mechanical origin of the evolution of the Biot coefficient of argilites during mechanical load. Scientific days, ANDRA 1999 Summary of communications and poster communications, (p. 258). France
- Kong, X., Delshad, M., & Wheeler, M. F. (2015). History Matching Heterogeneous Coreflood of CO_2/Brine by Use of Compositional Reservoir Simulator and Geostatistical Approach. Society of Petroleum Engineers. doi:10.2118/163625-PA

Mechanical properties

Elastic moduli from triaxial testing

Static elastic moduli were measured using the multistage-triaxial loading test attained by increasing deviatoric stress under three different constant confining pressures (500 psi, 1000 psi, and 1500 psi). The static elastic moduli can be calculated with the following relationships:

$$E = \left.\frac{\partial \sigma_{axial}}{\partial \varepsilon_{axial}}\right|_{\sigma_{radial}} \quad ; \quad \nu = -\left.\frac{\partial \varepsilon_{radial}}{\partial \varepsilon_{axial}}\right|_{\sigma_{radial}}$$

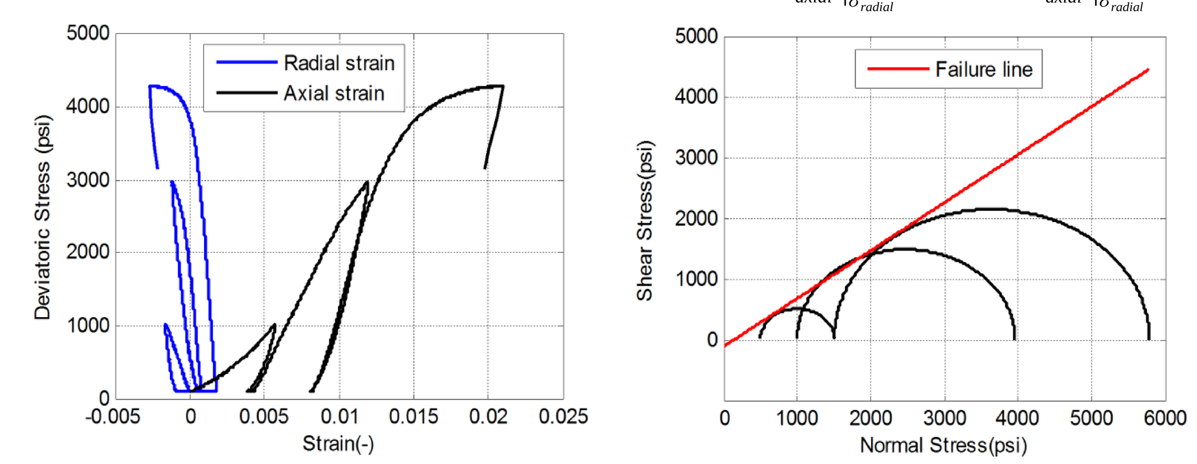

Fig. 4. Frio sandstone multi-stage triaxial testing at confining stress 500 psi, 1000 psi and 1500 psi: (left) Axial strain and radial strains measured for a single core plug, (right) Failure line at the onset of shear dilation.

Table 1. Static elastic moduli with different stress states

Confining pressure (psi)	Deviatoric stress, (psi)		E_{static} (GPa)	ν
500	Loading	91.5 - 276.2	0.82	0.21
	Loading	365 - 529	1.10	0.25
	Unloading	1025 - 809.7	7.21	0.35
1000	Loading	107.3 - 882.5	2.77	0.19
	Loading	1057 - 1506	2.74	0.18
	Unloading	2966 - 2364	8.47	0.42
1500	Loading	116.2 - 612.4	3.67	0.20
	Loading	1068 - 1904	5.46	0.29
	Unloading	4294 - 3839	8.04	0.33

Failure parameters from laboratory

From the onset of Figure 4 (right), the friction angle is about 38º and the cohesive strength is zero (this is unconsolidated sand).

Biot coefficient

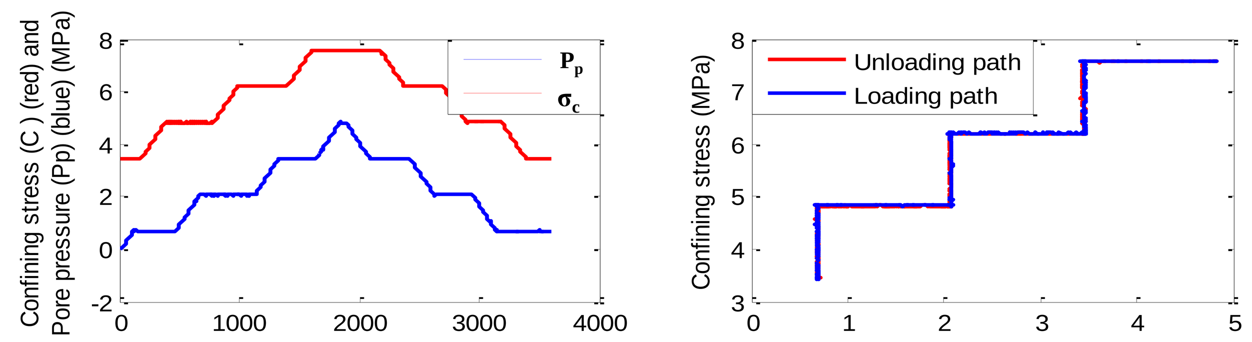

Fig. 5. Loading and unloading of confining stress (σ_c) and pore pressure (Pp)

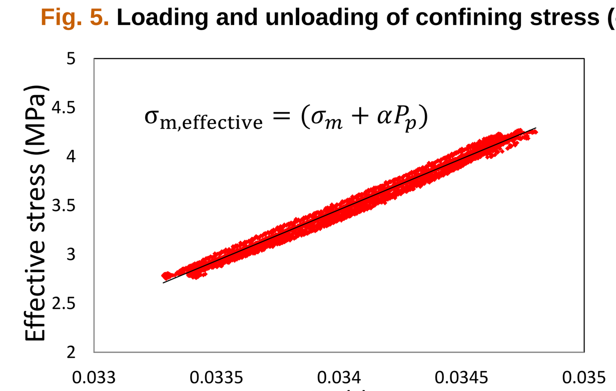

Fig. 6. Volumetric strain change as a function of Biot effective stress

Bulk Biot coefficient is measured by controlling confining stress and pore pressure step by step according to the procedure proposed by Bouteca et al. (1999) (Fig. 5.). The triaxial loading cell (Fig. 3.) is used to maintain stress condition and regulate pore pressure. The results show that the Biot coefficient for Frio sand is 0.97 (Fig. 6.).

Elastic moduli from well log analysis

Dynamic moduli (Young's modulus ($E_{dynamic}$) and Poisson's ratio ($\nu_{dynamic}$) were calculated with the Frio injection well logging data for Frio C sandstone interval (Raw data courtesy of the Gulf Carbon Center). Figure 7 shows the calculated values and measured logging data, which are required for the calculation.

$$E_{dynamic} = 2\rho V_s^2 (1+\nu); \quad \nu_{dynamic} = \frac{V_P^2 - 2V_S^2}{2V_P^2 - 2V_S^2},$$

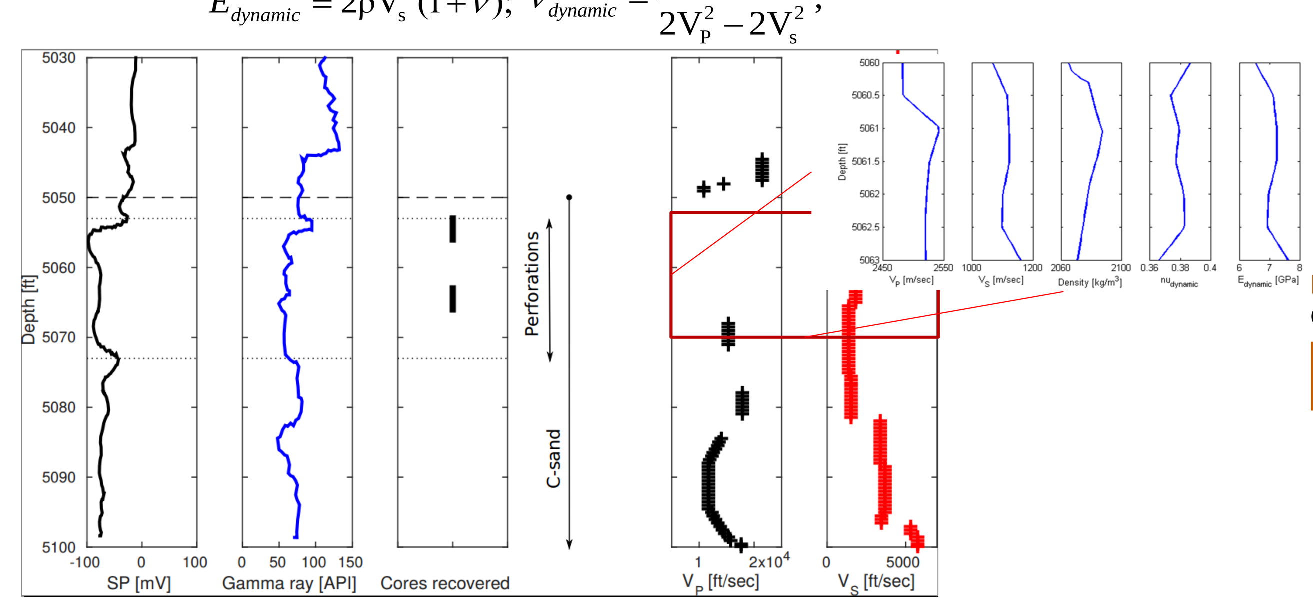

Fig. 7. Acoustic velocities and density measured by logging and calculated dynamic moduli of Frio C in injection well.

Petrophysical properties

Porosity

The calculated porosity for each sample is reported in Table 2.

Table 2. Calculated porosity of Frio samples

Sample number	V1	V3	H1	Average
Porosity	0.376	0.355	0.357	0.363

Permeability

Water and gas (N_2) permeabilities were measured at reservoir in-situ stress condition. The applied stress conditions are closely adjusted according to the core depth and in-situ lateral stresses.

Table 3. Measured permeability at reservoir stress condition

Sample number	k (mD)	k_g at breakthrough (mD)	k_w at S_{gr} (mD)
V1	470	184	263

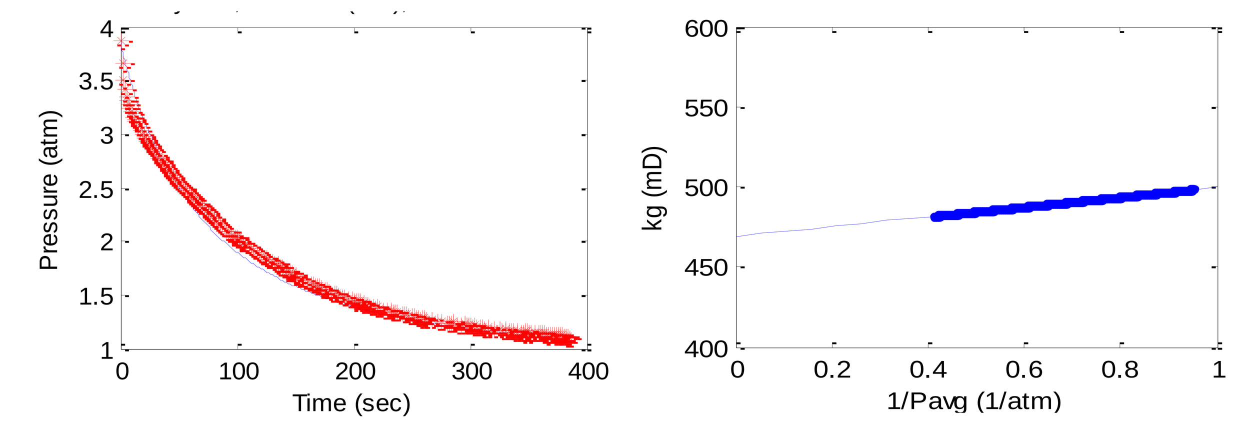

Fig. 8. Measured gas absolute permeability

Capillary pressure and relative permeability

Capillary pressure was measured with the air-brine porous-plate method and with mercury injection capillary pressure (MICP) method (Figure 9). CO_2-water capillary pressure at in-situ conditions are expected to be about one-third of the N_2-water capillary pressure measured in these tests. Relative permeability is calculated by Brooks-Corey model into MICP measurement. The parameters for Brooks-Corey model are in Table 4.

$$Pc = Pe * (S_w^*)^{\left(-\frac{1}{\lambda}\right)}; \quad S_w^* = \frac{S_w - S_{wir}}{1 - S_{wir}}$$

Table 4. Brookes-Corey model parameters for Frio C sandstone

λ	$\ln P_e$	P_e	K_{r_nw}	S_m
4.741584	0.4595	1.583282	0.82	0.95

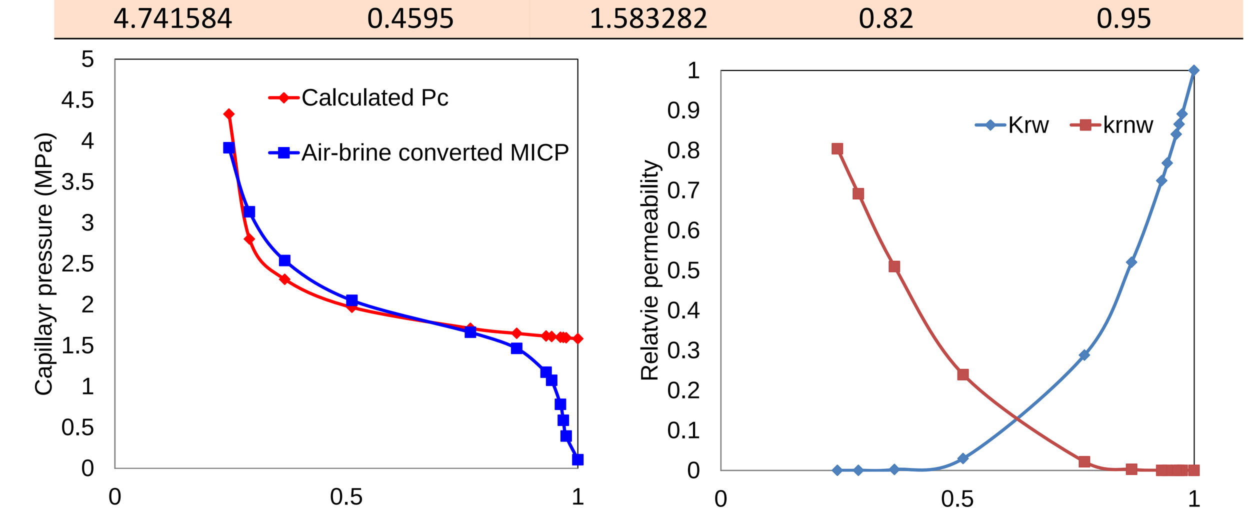

Fig. 9. Fitted MICP experiment result with Brookes-Corey model and (b) relative permeability curves of Frio C sandstone

Porosity and permeability from well log analysis

Since the Frio complex is highly laminated in sequences of sand and shaly sand, we used a linear correlation between sandstone and shale properties to correct shaliness and estimate porosity and permeability (Fig. 10).

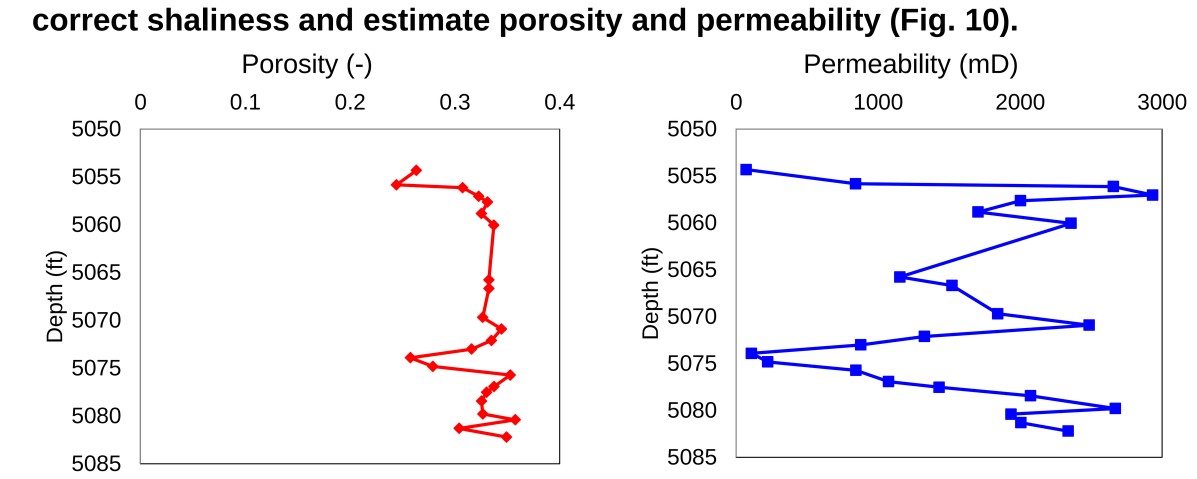

Fig. 10. Calculated porosity and permeability from well log analysis of Frio injection well before CO_2 injection.

Future work

- Experiments with rock specimens of different size (up to 4") to capture the effect of reservoir heterogeneity in effective properties.
- Measurement of high pressure and high temperature (HPHT) mechanical properties with CO_2-specific loadings. The schematic diagram of experiment apparatus is in Figure 3.
- History matching of the bottom hole pressure field data by correcting pressure boundary condition.
- Large CO_2 injection reservoir simulation including poro-elasticity.

Computational simulation results

Frio pilot test

Approximately, 1,800 tons of CO_2 was injected for 10 days, and breakthrough occurred after 5 days of injection (Hovorka et al., 2006).

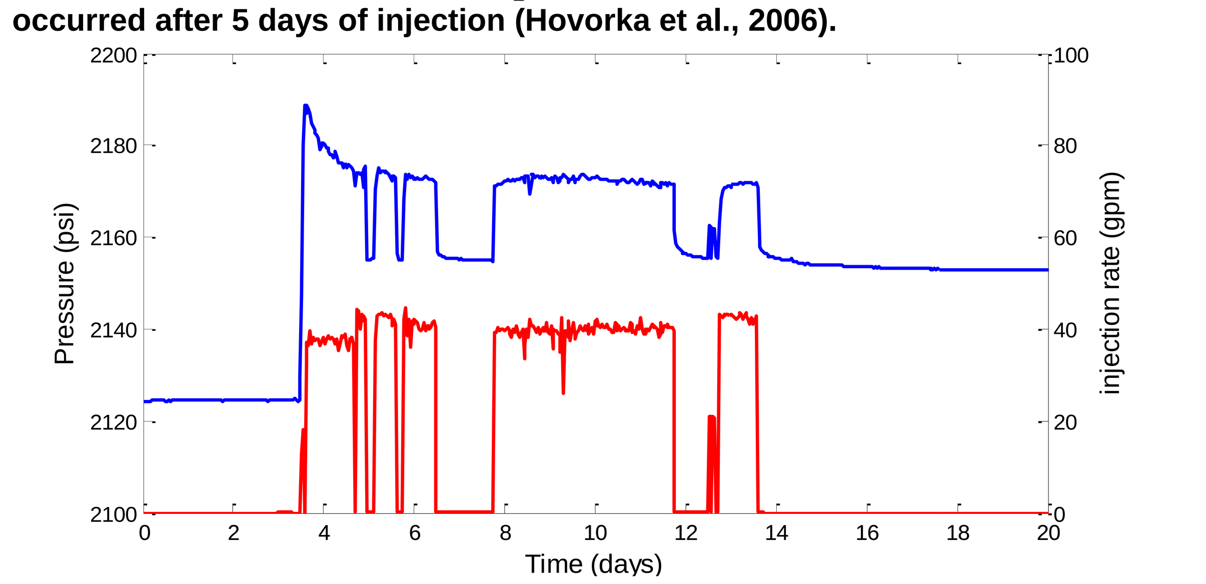

Fig. 12. Injection schedule of Frio "C"

Compositional fluid flow with fine scale reservoir setup

With the properties measured with experiments and well log analysis, a detailed Frio reservoir model is developed in our in-house reservoir simulator IPARs (Integrated Parallel Accurate Reservoir Simulator) to perform history matching for the pilot test. We located the injection and observation well at the right locations and inputted the correct injection schedule. The fine 2ft-scale permeability and porosity are assigned to the simulation (Figure 13). Capillary pressure and relative permeability are also assigned. The fluid properties are fine-tuned according to the Kong et al. (2015).

Table 5. Simulation input for compositional fluid flow simulation

Wells	1 injection well and 1 observation well
Injection well (1)-(6)	Volume Injection rate specified
Production (Observation) well (1)-(3)	Pressure specified rate (2190 psi)
Total simulation time	100 days
Number of grids (non-uniform grid size)	1.17E+5 grids (50*37*63)
Initial porosity (measured value from cored sample)	0.363
Initial reservoir pressure at the perforation depth	2190 psi
Rock compressibility	1.0E-6 (1/psi)

Table 6. Simulation input for compositional fluid flow simulation

NAME	TC (Rº)	Critical Pressure (psi)	Critical Z	Accentric factor (lbM/cu-ft)	Molecular weight	Parachor	Vshift	CP	CV
CO_2	547.56	1070.38	0.3023	0.224	44.01	49	-0.19	14.89	12.91
BRINE	1165.23	3203.88	0.2298	0.244	19.35	52	0.095	17.82	15.83

Figure 13 shows the CO_2 saturation along the reservoir after 30 days of the injection. The injection schedule and bottom hole pressure response are shown in Figure 14. The extra fine-tuned history matching will be performed.

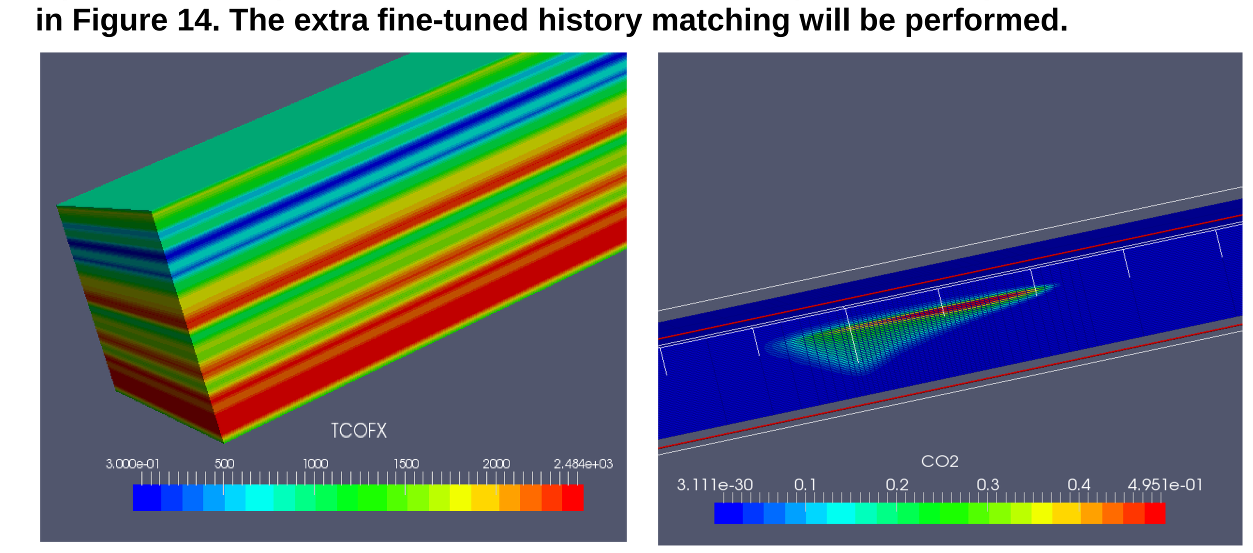

Fig. 13. Simulation input 2 ft-scale permeability (left) and CO_2 saturation in the middle of simulation (right)

No-flow boundary condition results in the increased bottom hole pressure; it will be corrected by locating multiple pressure specified production well.

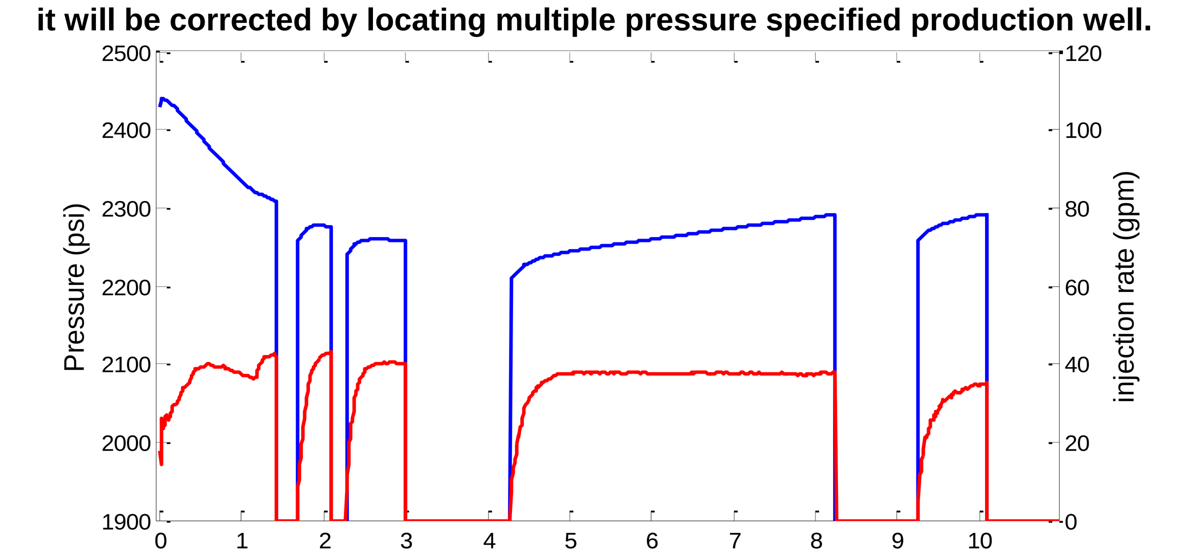

Fig. 14. Simulation results of bottom hope pressure (blue) and injection rate (red) at the injection well

Acknowledgements

The authors would like to thank DOE grant DE-FE0023314. The authors would like to express appreciation to Dr. Hovorka and BEG for sharing field data.